UNITED STATES DEPARTMENT OF THE INTERIOR
GEOLOGICAL SURVEY

RESULTS AND INTERPRETATION OF EXPLORATORY DRILLING
NEAR THE PICACHO FAULT, SOUTH-CENTRAL ARIZONA

By

Thomas L. Holzer

Open-File Report 78-1016

This report is preliminary and has not been edited
or reviewed for conformity with Geological Survey
standards and nomenclature

December 1978

CONTENTS

ILLUSTRATIONS

TABLES

Abstract

Modern surface faulting along the Picacho fault, east of Picacho,

Arizona, has been attributed to ground-water withdrawal. In September

1977, three exploratory test holes were drilled 5 km east of Picacho and

across the Picacho fault to investigate subsurface conditions and the

mechanism of the faulting. The holes were logged by conventional geophysical

and geologic methods. Piezometers were set in each hole and have been moni-

tored since September 1977. The drilling indicates that the unconsolidated

alluvium beneath the surface fault is approximately 310 m thick. Drilling and

piezometer data and an associated seismic refraction survey indicate that the

modern faulting is coincident with a preexisting, high-angle, normal fault

that offsets units within the alluvium as well as the underlying bedrock.

Piezometer and neutron log data indicate that the preexisting fault behaves as

a partial ground-water barrier. Monitoring of the piezometers indicates that

the magnitude of the man-induced difference in water level across the pre-

existing fault is seasonal in nature, essentially disappearing during periods

of water-level recovery. The magnitude of the seasonal difference in water

level, however, appears to be sufficient to account for the modern fault off-

set by localized differential compaction caused by a difference in water level

across the preexisting fault. In addition, repeated level surveys since

September 1977 of bench marks across the surface fault and near the piezometers

have indicated fault movement that corresponds to fluctuations of water level.

Introduction

Examples of surface faulting[1] possibly related to ground-water withdrawal from unconsolidated sediments have been recognized in several areas in the United States (Van Siclen, 1967; Rogers, 1967; Clark and others, 1978; Holzer, 1978; Holzer and others, 1979). For most of these examples, the specific mechanism of faulting, if the modern movement is indeed man-induced, and subsurface conditions at the faults have not been studies in detail. As a consequence, it is not understood why such faulting occurs and what subsurface conditions are conducive to its occurrence. In order to understand subsurface conditions beneath one of these faults and to seek data that would contribute to the understanding of mechanisms for such faulting, a geophysical and drilling program was conducted. This report describes and interprets the results from the drilling program conducted in September 1977. Results from the geophysical investigation are published in Open-File Report 78-933 (Pankratz and others, 1978).

The Picacho fault, east of Picacho in south-central Arizona (see insert, fig. 1), was selected for detailed investigation because arguments have been made for a relation between modern fault offset and ground-water withdrawal (Holzer and others, 1979). These arguments, however, were based principally on geodetic data. Very little was known about detailed subsurface hydrologic and geologic conditions beneath the surface fault, although Schumann and Poland (1971, p. 299-300) implied, based on a regional gravity survey, that the surface fault might be underlain by a "buried fault scarp". Peirce (1976) also suggested that the eastern margin of the Picacho basin, along which the modern faulting occurs, in bounded by a preexisting fault zone.

_____

[1]Surface faulting is used here to characterize failure of the land surface in which points at the land surface on opposite sides of the failure plane move parallel to the failure plane.

The Picacho fault at the surface consists of a 15.8 km-long scarp that

ranges from 0.2 to 0.6 m high (Holzer and others, 1979). Geodetic data

indicate the modern faulting is high-angle and normal (Holzer and Thatcher,

1979). The fault occurs near the eastern margin of the Eloy-Picacho subsidence

bowl at the center of which more than 3.8 m of subsidence has been caused by

ground-water level declines (Laney and others, 1978). The subsidence bowl is

restricted to an alluvial basin containing unconsolidated sediments bounded by

crystalline bedrock that crops out discontinuously around the basin. The hydro-

geology of the basin was described by Hardt and Cattany (1965).

Location

Three exploratory test holes were drilled approximately 5 km east of

Picacho, Arizona in T8S, R9E, section 20 (fig. 1). The holes were drilled

adjacent to a dirt road that trends northwest through section 20 from its

southeast corner and intersects the Picacho fault at an angle of 55°. Two test

holes were drilled on the downthrown side of the fault scarp, (D-8-9) 20BDA[1]

and (D-8-9) 20BAC[1], 28 and 246 m respectively, from the scarp as measured along

the dirt road. As measured normal to the scarp, these two test holes are 23

and 201 m respectively from the scarp. A third test hole, (D-8-9) 20BDD[1] was

drilled 176 m from the scarp on the upthrown side as measured along the dirt

road or 143 m from the scarp measured normal to the scarp. The drilling sites

were selected because of accessibility and their proximity to a survey line

with a long history of repeated surveys that crosses the fault (Holzer and

others, 1979). The survey line also permitted precise determination of the

absolute elevation of the land surface at each drill site.

---

[1] Test hole numbers are in accordance with the convention used in Arizona by the
Water Resources Division of the U.S. Geological Survey (see e.g., Babcock, 1973,
p. 4).

Methods

Three 12 cm-diameter test holes were drilled by conventional rotary-drilling method with mud for a drilling fluid to approximately 15 m beneath the base of the unconsolidated alluvium. Cuttings were collected every 3 m and were analyzed in a lab for grain-size distribution. In addition, drilling conditions were continuously monitored by professional geologists and a record of drilling speed based on 3-m increments was kept manually. Upon completion of drilling, geophysical logging - including neutron, gamma-gamma, natural gamma, electric, and caliper logs - was conducted by the Hydrologic Equipment and Services Unit of the U.S. Geological Survey.

Piezometers were subsequently installed in each hole at a depth of approximately 231 m. Each piezometer consisted of a 3.2 cm-diameter black steel casing attached to a 1.5 m length of stainless steel, 8-slot, well screen with a 1.5 m sump at its base. The piezometers, after adverse experience in the first hole, (D-8-9) 20BDD, were developed by flushing clear water out through the well screen before any backfill was placed in the hole. Flushing was continued until clear water flowed up out of the borehole annulus at the surface. Holes were then backfilled with pea gravel from the surface by washing the pea gravel down the hole.

Test hole (D-8-9) 20BDD was cored every 15.2 m from 30.5 to 121.9 m with a 6.35 cm-diameter by 3 m-long spot core sample barrel. Samples, all of unconsolidated alluvium from each core, were analyzed for Atterberg limits, linear shrinkage, grain-size distribution, and clay mineralogy of the clay fraction. In addition, bedrock at the base of test hole (D-8-9) 20BDA was cored.

Results - Physical Properties

Test Hole (D-8-9) 20BDD

Test hole (D-8-9) 20BDD, on the upthrown side of the fault scarp, was drilled to a depth of 304.5 m. Drilling progressed rapidly at an approximately constant rate, except for interruptions for coring, to a depth between 292.6 and 295.7 m (fig. 2). Above this depth, cuttings, cores (table 1) and geophysical logs (pl. 1) indicated a heterogeneous, brown, clastic sedimentary deposit of moderate porosity with individual units ranging from predominantly clay to coarse sand. This material presumably is unconsolidated alluvium. No clear-cut subdivision of the alluvial portion of the test hole into separate stratigraphic units appeared feasible. Both the resistivity and neutron logs (pls. 1A and 1B) indicated that individual beds were typically less than 3 m thick. Grain-size analyses of cuttings (table 2 and fig. 3) suggest that the deposit becomes coarser with depth. This coarsening with depth appears to be reflected by the nuclear logs. The gamma-gamma log (pl. 1C) shows a step-wise increase in density at a depth of 230 m. The change in the neutron log (pl. 1B) is more gradual with a transitional decrease of porosity occurring from 183 to 198 m.

Within the depth interval 292.6 to 295.7 m the rate of penetration decreased significantly and remained low to the bottom of the hole (fig. 2). Cuttings from below 295.7 m consisted of coarse angular grains of predominantly gneiss, quartz, and feldspar. Inspection of the drill bit after its recovery indicated a very abrasive formation in the deeper part of the hole. The characters of the resistivity and the neutron logs change at a depth of approximately 294 m, indicating a resistive material with relatively low porosity below this depth. The gamma-gamma log indicates that the material with the lower porosity also has a slightly higher bulk density relative to the shallower material. The

actual contact between the deep and shallow units, however, may not be as clear-cut as the drilling behavior suggests. At a depth of 286.2 m, a 3.7 m-thick stratum was encountered that has a very high porosity and low-bulk density relative to the shallow unit. Although it might be natural to include this stratum in the shallower unit, its natural gamma radiation corresponds much more closely to the deeper unit.

The neutron and gamma-gamma logs indicate that very dense material with a porosity of nearly zero was penetrated for approximately 2.9 m below a depth of 301.6 m. The resistivity and spontaneous potential logs also suggest material with different physical characteristics was penetrated in this interval. The natural gamma radiation of this material is similar to that of the material immediately overlying it.

Test Hole (D-8-9) 20BDA

Test hole (D-8-9) 20BDA, 23 m from the fault scarp on the downthrown side, was drilled to a depth of 323.1 m. The test hole was purposely located close to the scarp in an attempt to drill through the fault at depth. Drilling progressed rapidly until circulation was partially lost at a depth of approximately 99 m. Circulation loss continued intermittently to a depth of 106.7 m where it became necessary to stop drilling operations because an estimated 2000 to 3000 gallons (7.6 to 11.4 cu. m) of drilling fluid had been lost. A denser drilling fluid was then mixed, and drilling was resumed and continued to a depth of 176.7 m where, because of continued loss of drilling fluid, the test hole was "dry packed" with cotton seed hulls. This was completed with the drill bit at a depth of 183 m. Subsequently, drilling progressed at a rapid rate to approximately 315 m, at which depth the rate of penetration diminished significantly (fig. 5). Intermittent shaking of the drill string began at a depth of approximately 306 m precursory to the decrease of the rate of penetration. Inspection of the drill bit again indicated a very abrasive formation.

Above a depth of 306 m, cuttings and geophysical logs (pl. 2) indicate that a sedimentary deposit similar to that in the upper part of test hole (D-8-9) 20BDD was encountered. An increase in the percentage of fine-grained material in the cuttings from 119 to 213 m (fig. 6) may be due to the increase in drilling mud density that was done to reduce circulation loss. The precise depth of the base of the unconsolidated alluvial deposit is indicated by the neutron and resistivity logs, which show an abrupt change at a depth of 305.2 m to a more resistive material with a relatively lower porosity (fig. 7). The decrease in porosity is accompanied by an increase in bulk density according to the gamma-gamma log and a slight decrease of natural gamma radiation

7

from the formation (fig. 7). The cuttings also are compatible with a contact at 305.2 m. Below this depth, particles were predominantly coarse-grained and were very angular as contrasted with more rounded particles in the shallower material.

The dense, low-porosity material overlying the contact that was observed in (D-8-9) 20BDD is not as well defined in (D-8-9) 20BDA, and may in fact be absent. Material with properties somewhat similar to the interval 286.2 to 289.9 m in test hole (D-8-9) 20BDD was observed from 301.6 to 305.1 m. The correlation, however, is tenuous.

Both the neutron and gamma-gamma logs indicate that below a depth of 319.4 m approximately 3.7 m of very dense material with very low porosity was penetrated. The material seems to be the same as encountered at the bottom of (D-8-9) 20BDD because the characteristics of the resistivity and spontaneous potential logs are similar between the two holes. The natural gamma radiation of the deep material in (D-8-9) 20BDA is similar to that of the overlying dense, low-porosity material. The bottom of the test hole was cored, and approximately 0.3 m of broken gneissic crystalline rock fragments filled the bottom of the core barrel. The fragments ranged from 20 to 60 mm in diameter. Thin sections were made of the five fragments that appeared to be the most dissimilar. All five thin sections revealed that the cored material was biotite quartz monzonite with thin layers of annealed polycrystalline quartz, indicating that the rock had been subjected to tectonic shearing.

Test Hole (D-8-9) 20BAC

Test hole (D-8-9) 20BAC, 201 m from the fault scarp on the downthrown side, was drilled to a depth of 362.7 m. Drilling progressed at a rate approximately equal to that of the other two test holes until at a depth between 347.5 and 350.5 m the rate of penetration decreased (fig. 8). Above these depths, cuttings and geophysical logs (pl. 3) indicated a sedimentary deposit similar to that inferred to be unconsolidated alluvium in test hole (D-8-9) 20BDD. Cuttings from depths ranging from 274.3 to 335.3 m indicated that a fine-grained unit was present (table 2 and fig. 9). None of the geophysical logs, however, indicated any characteristics that distinguish this interval from the remaining portion of the alluvial section. The log of natural gamma radiation indicates the presence of two approximately 6 m-thick intervals with natural gamma radiation exceeding 110 cps (counts per second) at depths of 272.5 and 291.7 m (pl. 3D).

The geophysical logs (fig. 10) correlate quite well with the drilling behavior. The resistivity and neutron logs indicate a contact between the overlying alluvium and a more resistive, low-porosity material at 349.6 m. The contact is somewhat gradational on the neutron log with the gradation beginning at 340.2. As in the two other holes, the deeper material has a higher bulk density and lower natural gamma activity relative to the overlying material.

The low-density and high-porosity material above the contact indicated by the gamma-gamma and neutron logs is probably due to a localized increase in the diameter of the bore hole and probably does not reflect actual material properties.

9

Unlike the previous two holes, the test hole did not penetrate a dense, nonporous material at the bottom. The hole was completed in the same material that was encountered beginning at a depth of 349.6 m.

Results - Hydrologic Data

Repeated measurements of water levels in the piezometers set in each of the test holes and neutron logs obtained after drilling are available to evaluate ground-water conditions at the surface fault. The data are summarized in table 3.

All three piezometers were set at the same depth, approximately 231 m (table 3), to minimize possible effects from vertical variations of fluid potential. Each piezometer was tested by the slug method, and response times were determined to be less than one day for the piezometers in test holes (D-8-9) 20BDA and 20BAC. The piezometer in test hole (D-8-9) 20BDD initially was plugged, but was finally successfully developed by the U.S. Bureau of Reclamation in the summer of 1978.

The neutron logs revealed a well-defined top to the zone of saturation in each of the test holes (fig. 11). The logs also indicated that a considerable amount of soil moisture has been retained in the part of the deposit dewatered by ground-water withdrawal.

Interpretation of Results

The preferred interpretation of the drilling and hydrologic data is shown in cross section in figure 12. The cross section is a projection passing through (D-8-9) 20BDA normal to the strike of the fault. The contact between the alluvium and unit B in figure 12 is based on the resistivity and neutron logs, which indicated a marked increase in resistivity accompanied by a decrease in porosity near the bottom of each test hole. Unit C in test holes (D-8-9) 20BDA and 20BDD is the very dense, nonporous material encountered beneath unit B at the bottom of each of these two test holes. The upper surface of unit B presumably is the base of the compacting alluvial material causing land subsidence near the fault, since the properties of units B and C inferred from the geophysical logs and their drilling resistance indicate material which is relatively incompressible. Unit B and material beneath it will henceforth be referred to as "hydrologic bedrock". A preexisting, high-angle, normal fault offsetting alluvium and underlying hydrologic bedrock and behaving as a partial ground-water barrier is interpreted to connect to the modern surface fault. The magnitude of fault offset at the base of the alluvium, estimated to be approximately 30 m in the cross section, is based on assuming the bedrock surface has the same slope on both sides of the fault. Hence, the estimate of the amount of offset is somewhat arbitrary. The dip of the fault in the cross section is based on connecting the surface fault with the point in (D-8-9) 20BDA at which circulation loss began. Interpretation of a preexisting fault is based principally on geophysical and hydrologic data since no stratigraphic correlations within the alluvium were made. Although the tectonic shearing of the rock cored at the base of (D-8-9) 20BDA suggests at least the possibility of a preexisting fault zone within the hydrologic bedrock.

11

The seismic refraction investigation by Pankratz and others (1978) indicated that the alluvium beneath the Picacho fault is underlain by material at a depth of approximately 310 m that undergoes a velocity transition approximately beneath the surface fault. This material probably is unit B. The seismic velocity changes from 3.7 to 3.0 km/s in a westerly direction in the vicinity of the surface fault. In addition, at a depth of 800 m on the downthrown side of the surface fault, they interpreted a 100 m offset of a layer with an average velocity of 5.5 km/s. These results indicate the probability of high-angle, normal faulting within the hydrologic bedrock that underlies the alluvium beneath the modern scarp.

Projection of this fault into the alluvium and its connection to the modern fault scarp is based principally on hydrologic data. Although the increase of thickness of alluvium between test holes (D-8-9) 20BAC and 20BDA relative to the thickness based on a projection from (D-8-9) 20BDA and 20BDD suggests the possibility of offset in the hydrologic bedrock surface. The strongest hydrologic evidence for a preexisting fault within the alluvium is the water levels measured on September 17-18, 1978. The water level in the piezometer interpreted to be on the downthrown side of the fault was much lower than the water level projected from the two piezometers interpreted to be on the upthrown side of the fault (table 3 and fig. 12). This difference suggests the possibility of a partial ground-water barrier between piezometers (D-8-9) 20BAD and 20BDA. The absence of a conspicuous barrier effect in the September 30, 1977, and April 19, 1978, measuremtns could be caused by the seasonal nature of ground-water withdrawal in the area (Schumann and Poland, 1971, p. 297-298) and the restriction of all of the production wells to the west side of the fault. Under such conditions one would anticipate that seasonal fluctuations would be greatest on the west side of the fault and the magnitude of the

water-level difference would tend to diminish during periods of water-level recovery. Only if the fault were a completely impermeable barrier and there were no source of recharge, including delayed drainage, to the aquifer, would one anticipate that the difference in water-levels would be maintained year-round. The inferred seasonal fluctuation is supported by monthly measurements of water levels in the piezometers by the University of Arizona (S. N. Davis, oral commun., 1978).

Results from the neutron logs are compatible with the interpretation of a partial ground-water barrier within the alluvium. If the preexisting fault plane intersects test hole (D-8-9) 20BDA where circulation was lost, then the saturation of the material beneath this depth could be attributed to the fault behaving as a ground-water barrier. Attributing the saturation to penetration of drilling fluid does not appear to be satisfactory because there is no indication based on the neutron log of unsaturated material beneath this zone and it would seem to be fortuitous that the drilling fluid would have completely saturated material down to the top of the zone of saturation. In addition, the seismic refraction survey by Pankratz and others (1978) supports the former interpretation of the neutron logs. They found that a layer with a velocity ranging from 1.9 to 2.0 km/s dropped 28 m in elevation to the west beneath the fault at a depth of approximately 90 m. The velocity of the material overlying this layer ranges from 0.98 to 1.1 km/s. These velocities suggest that the upper surface of the 1.9 to 2.0 km/s layer is the contact between unsaturated and saturated alluvium.

Discussion

A preexisting fault behaving as a partial ground-water barrier could account for the history of ground failure and surface deformation across the Picacho fault. Previously, Holzer and others (1979) argued that modern surface faulting was preceded by differential subsidence across a narrow zone. A fault-controlled partial ground-water barrier could account for the localized differential subsidence by differential compaction. The presence of a partial ground-water barrier could also account for the fissuring (long, open tension cracks with no vertical offset) beginning in 1949 that preceded the surface faulting which began in 1961. Holzer (1977, fig. 1) previously inferred that differential subsidence from 1934 to 1949 of bench marks 8.6 km apart that spanned the earth fissure in 1949 was less than 15 cm. He noted that the magnitude of that differential subsidence appeared to be too small to generate significant horizontal tensional strains. If, however, most of the differential subsidence were localized across a preexisting fault (by differential water-level declines), then it is conceivable that horizontal tensional strains sufficient to cause fissuring may have been locally generated. Water-level declines of approximately 20 m in 1949 (based on spring measurements) on the west side of the fissure were inferred by Holzer and others (1979, fig. 3B). By this explanation, the eventual evolution of the earth fissure into a surface fault is explained by the differential compaction ultimately attaining a magnitude sufficient to cause shear failure.

Emplacement and monitoring of the piezometers near bench marks GMC-6 and 7 (fig. 1) has permitted a more controlled study of the relation between water-level fluctuations and fault movement than heretofore possible. Holzer (1977, fig. 3) concluded that movement of the Picacho fault at the bench marks was seasonal, at least from 1964 to 1968. Repeated leveling of these marks

14

beginning in September 1977 along with the monitoring of water levels confirms
that seasonal movement of the fault is still occurring (fig. 13). Fault
movement, as recorded by surveys of bench marks GMC-6 and 7 which span the
fault and are 14.5 m apart, corresponds to the fluctuation of water-level in
piezometer (D-8-9) 20BAC on the downthrown side of the fault. This result
provides additional support for a relation between modern surface faulting
and ground-water withdrawal.

Acknowledgments

References

Babcock, H. M., 1973, Annual report on ground water in Arizona, Spring 1971

    to Spring 1972: Arizona Water Commission Bulletin 5, p. 4.

Clark, M. M., Buchanan-Banks, J. M., and Holzer, T. L., 1978, Creep along

    parts of the Garlock fault: possible relation to decline in ground-water

    levels [abs.]: Geological Society of America Abstracts with Programs,

    v. 10, no. 3, p. 100.

Hardt, W. F., and Cattany, R. E., 1965, Description and analysis of the geo-

    hydrologic system in western Pinal County, Arizona: U.S. Geological

    Survey Open-File Report, Tucson, Arizona, U.S. Geological Survey.

Holzer, T. L., 1977, Ground failure in areas of subsidence due to ground-water

    decline in the United States: International Association of Hydrological

    Sciences land subsidence symposium, 2nd Anaheim, Calif., 1976, Proceed-

    ings (Pub. no. 121), p. 423-433.

Holzer, T. L., 1978, Surface faulting probably related to ground-water with-

    drawal, San Joaquin Valley, California [abs.]: Geological Society of

    America Abstracts with Programs, v. 10, no. 7, p. 424.

Holzer, T. L., Davis, S. N., and Lofgren, B. E., 1979, Faulting caused by

    ground-water extraction in south-central Arizona: American Geophysical

    Union Journal of Geophysical Research (in press).

Holzer, T. L., and Thatcher, Wayne, 1979, Modeling deformation due to subsid-

    ence faulting: International Conf. on Evaluation and Prediction of

    Subsidence, Pensacola, Fla., 1978, Proceedings (in press).

Laney, R. L., Raymond, R. H., and Winikka, C. C., 1978, Maps showing water-

    level declines, land subsidence, and earth fissures in south-central

    Arizona: U.S. Geological Survey Water Resources Investigations 78-83.

Pankratz, L. W., Ackermann, H. D., and Jachens, R. C., 1978, Results and interpretation of geophysical studies near the Picacho fault, south-central Arizona: U.S. Geological Survey Open-File Report 78-933, Denver, Colorado, U.S. Geological Survey.

Peirce, H. W., 1976, Tectonic significance of basin and range thick evaporite deposits: Arizona Geological Society Digest, v. 10, p. 325-339.

Rogers, T. H., 1967, Active extensional faulting north of Hollister near the Calaveras fault zone: Seismological Society of America Bulletin, v. 57, no. 4, p. 813-816.

Schumann, H. H., and Poland, J. F., 1971, Land subsidence, earth fissures, and ground-water withdrawal in south-central Arizona, U.S.A., in Land Subsidence: Tokyo International Association of Scientific Hydrology, Pub. 88, v. 1, p. 295-302.

Van Siclen, D. C., 1967, The Houston fault problem: American Institute of Professional Geologists, Texas Section, Annual Meeting, 3rd, Dallas, Texas, 1967, Proceedings, p. 9-31.

T8S R9E Sec 20
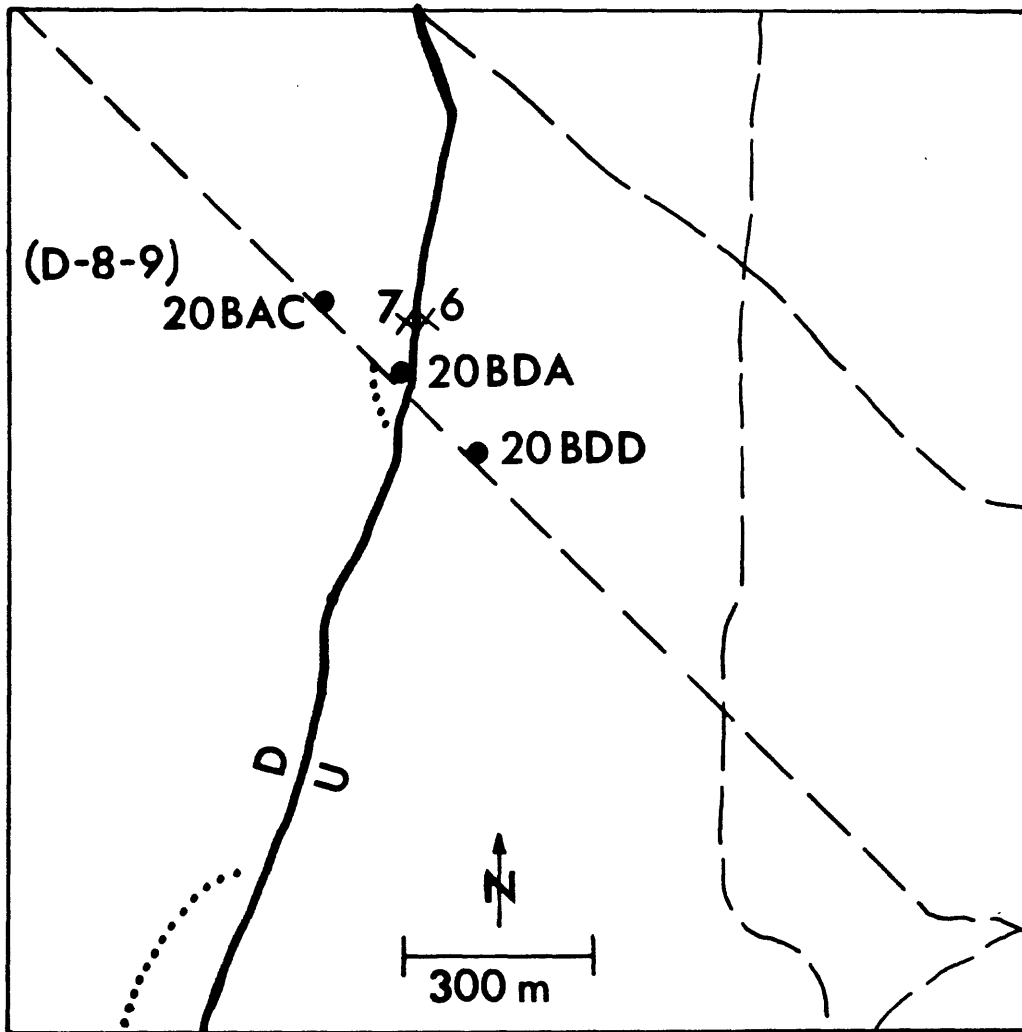
FIGURE 1.--Location map of exploratory test holes. Test holes are approximately 5 km east of Picacho, Arizona.
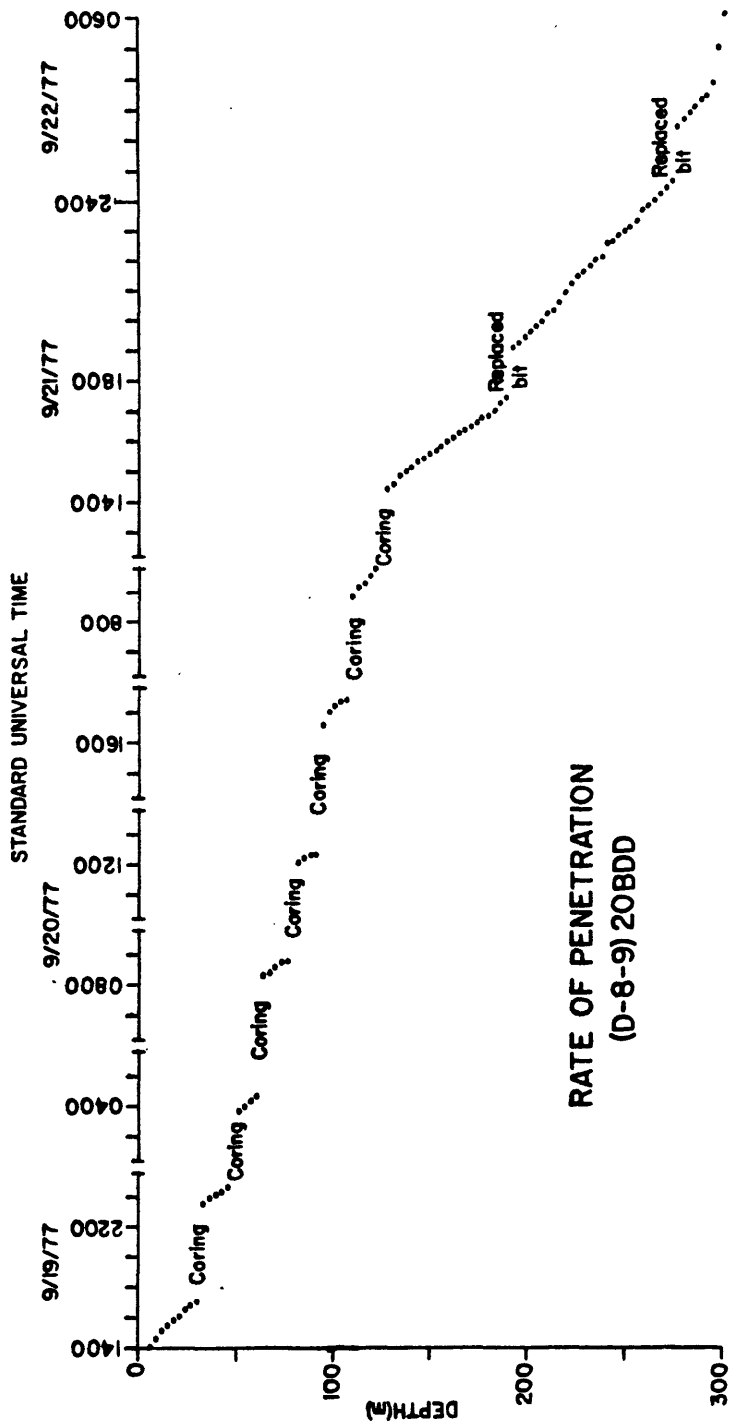
FIGURE 2.—Drilling penetration versus time, (D-8-9) 20BDD.

PERCENT LESS THAN 0.0625mm DIAMETER

(D-8-9) 20BDD

GRAIN-SIZE ANALYSIS
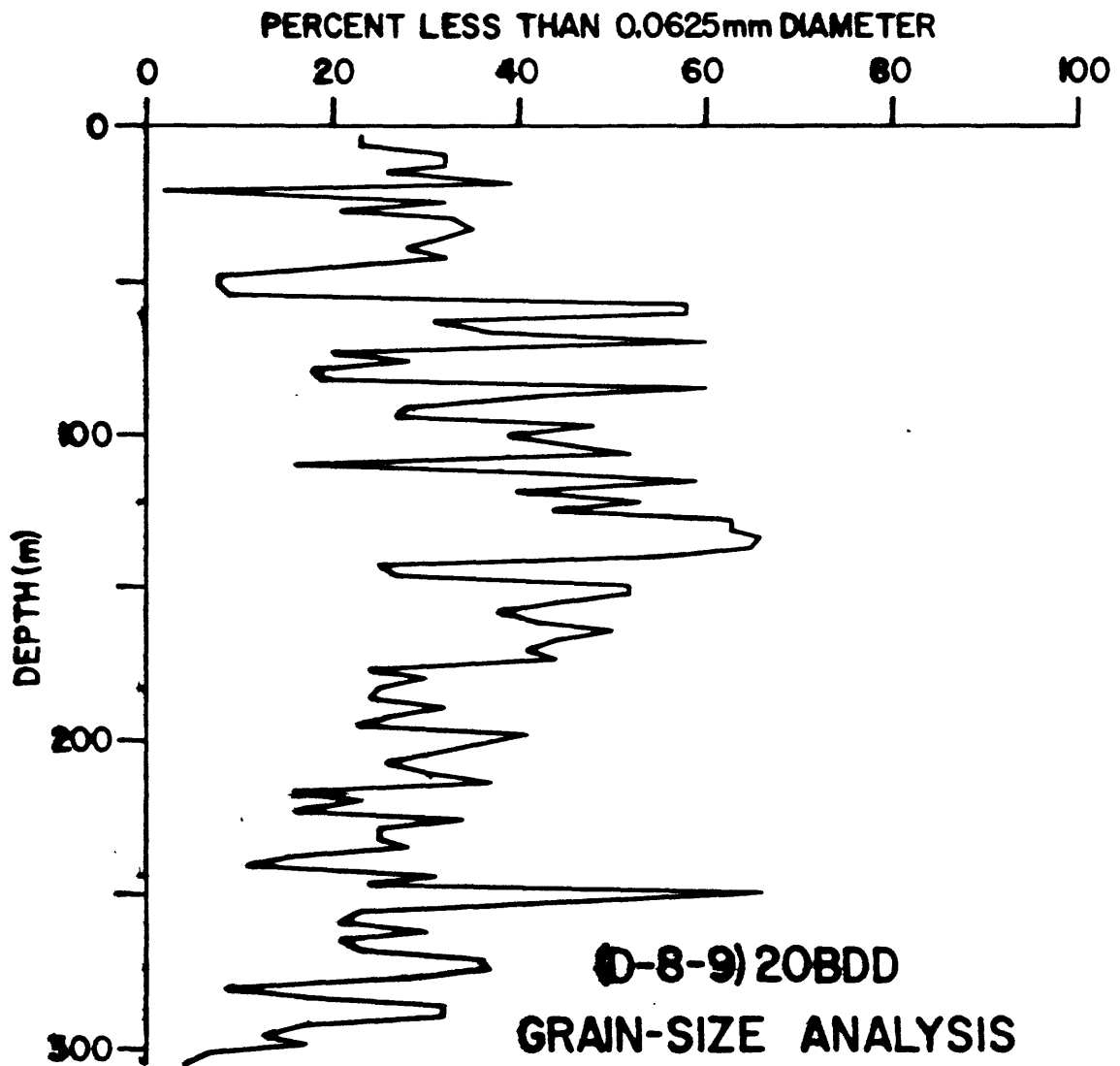
FIGURE 3.--Percent silt and clay in cuttings versus depth, (D-8-9) 20BDD.

GEOPHYSICAL LOGS (D-8-9) 20BDD
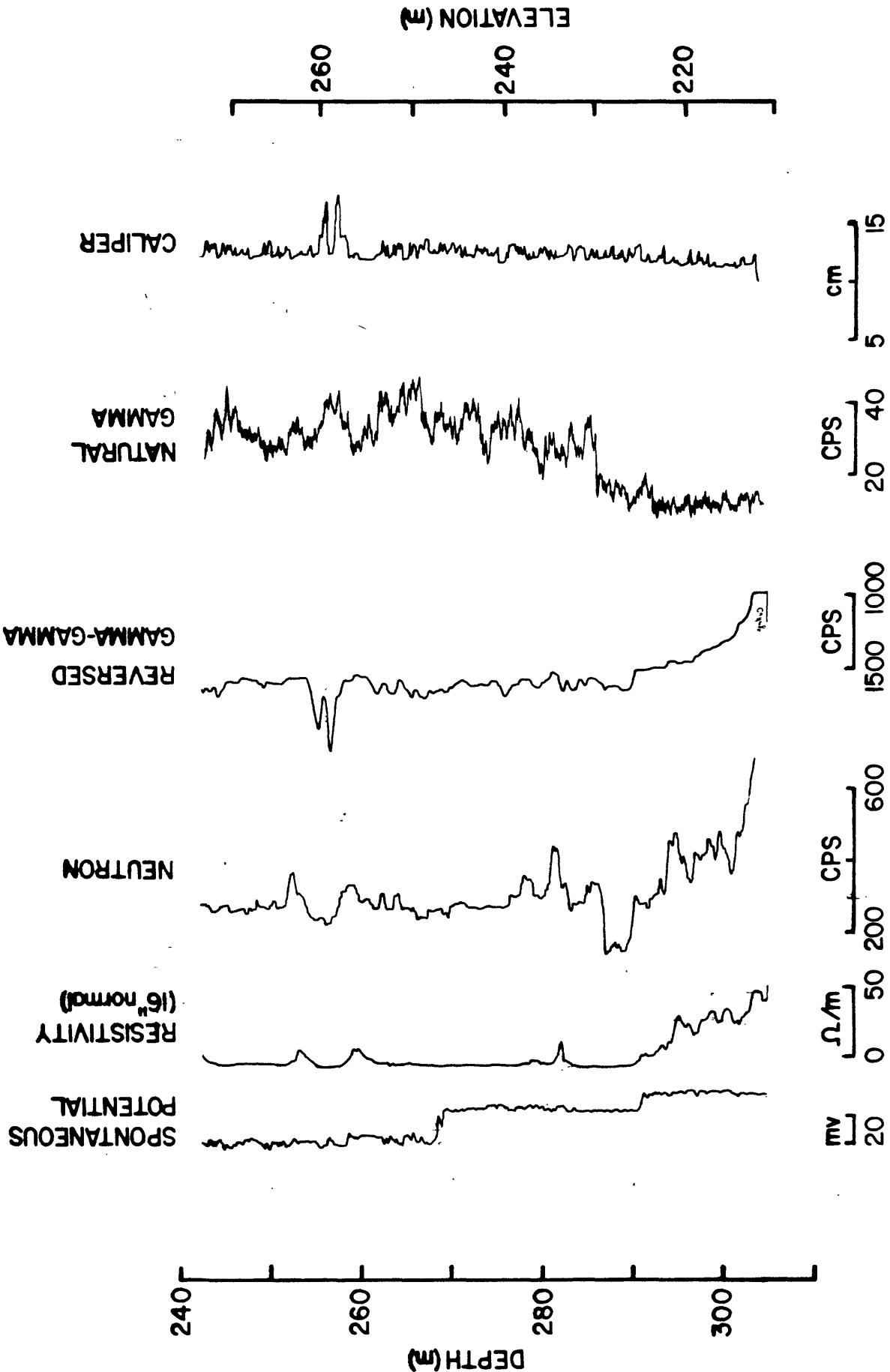
FIGURE 4.--Geophysical logs of lower part of (D-8-9) 20BDD.

21
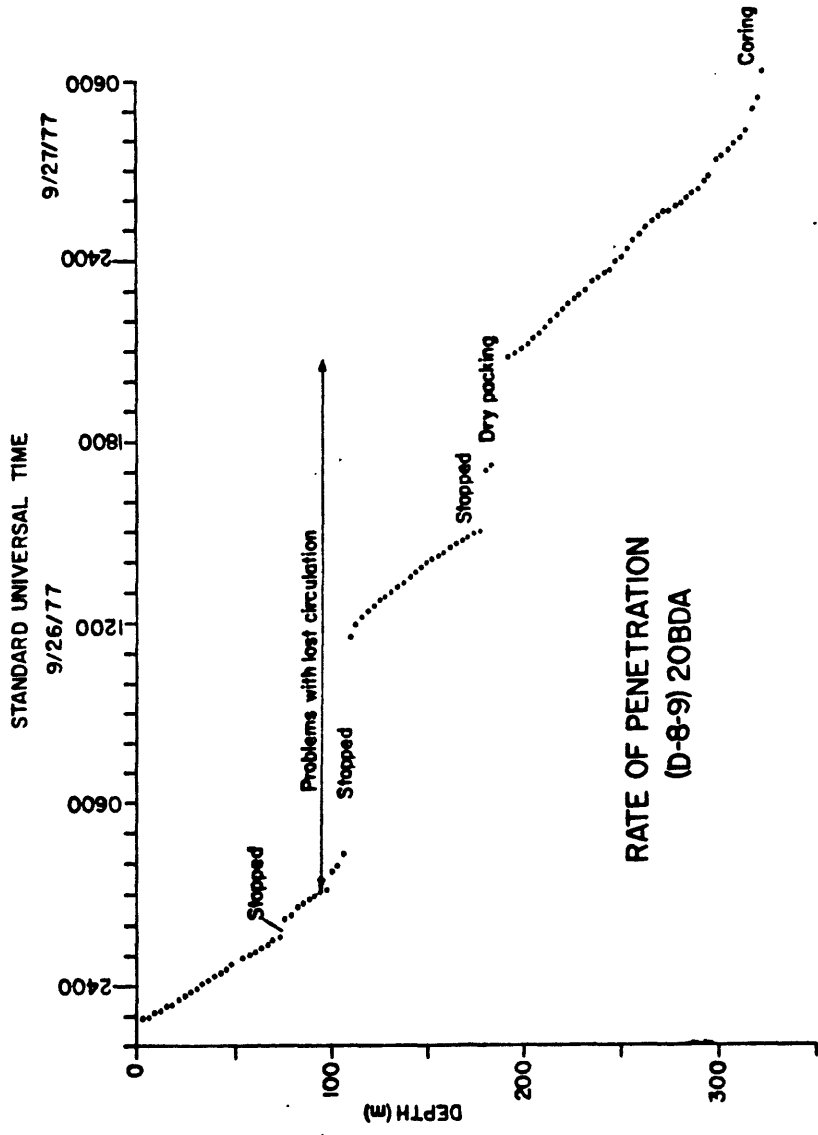
FIGURE 5.--Drilling penetration versus time, (D-8-9) 20BDA.

PERCENT LESS THAN 0.0625mm DIAMETER
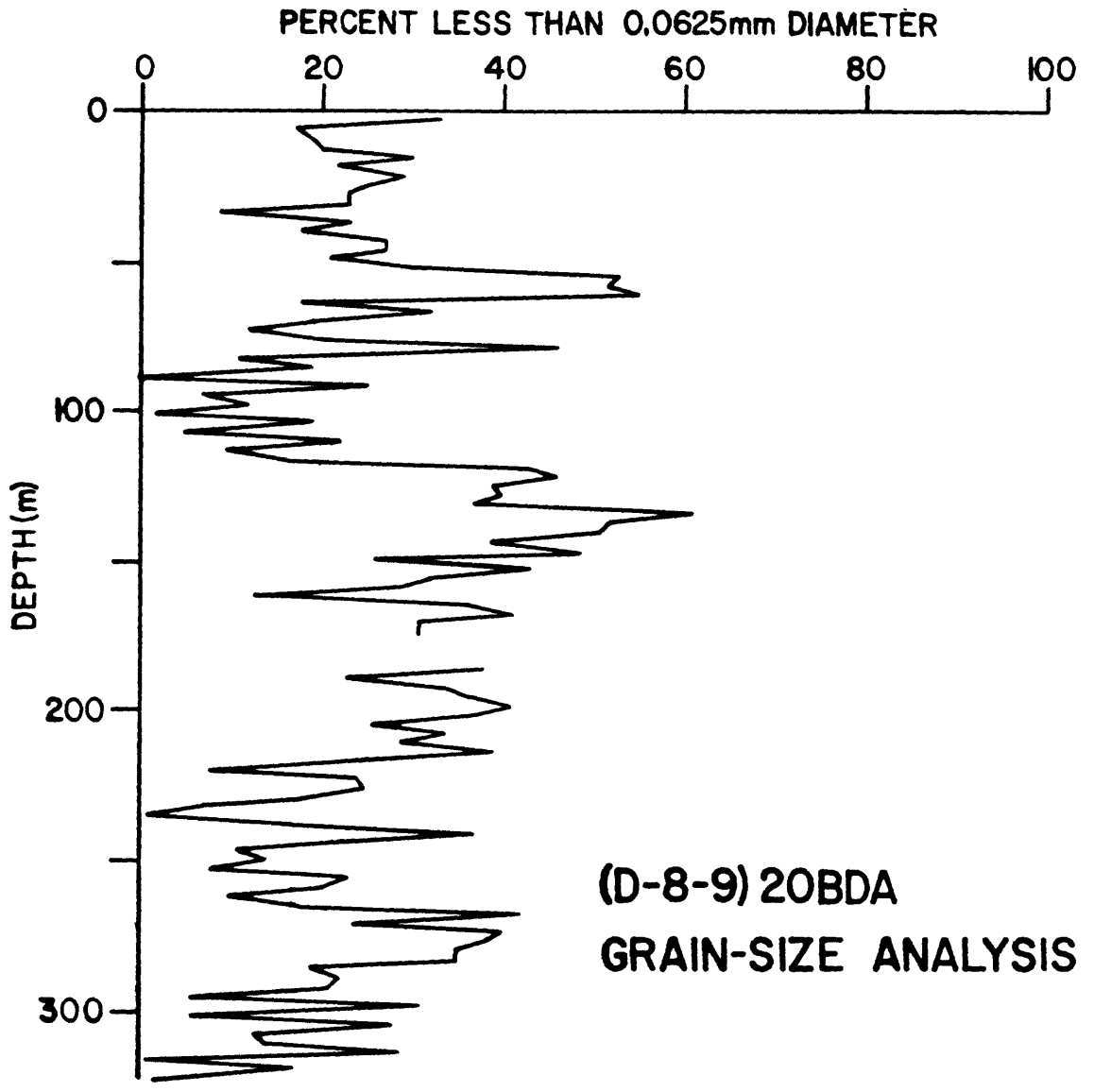
FIGURE 6.--Percent silt and clay in cuttings versus depth, (D-8-9) 20BDA.

GEOPHYSICAL LOGS (D-8-9) 20BDA

ELEVATION (m)

260   240   220   200

CALIPER   cm   15   10

NATURAL GAMMA   CPS   80   40

REVERSED GAMMA-GAMMA   CPS   2000   3000

NEUTRON   CPS   600   400

RESISTIVITY (1.5_M normal) Ω/m 50   0

SPONTANEOUS POTENTIAL   mv   20

DEPTH (m)

260   280   300   320
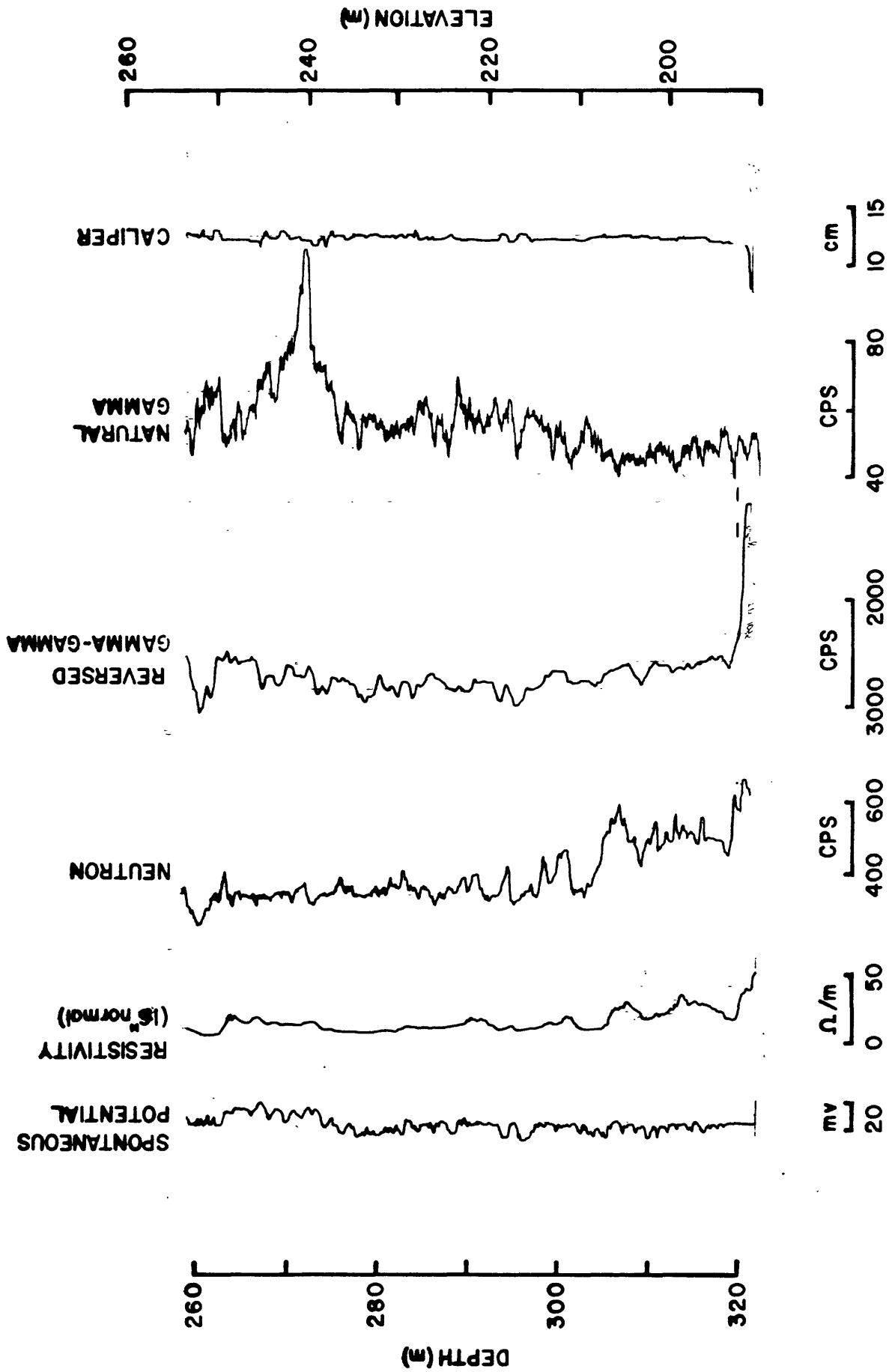
FIGURE 7.--Geophysical logs of lower part of (D-8-9) 20BDA.

24
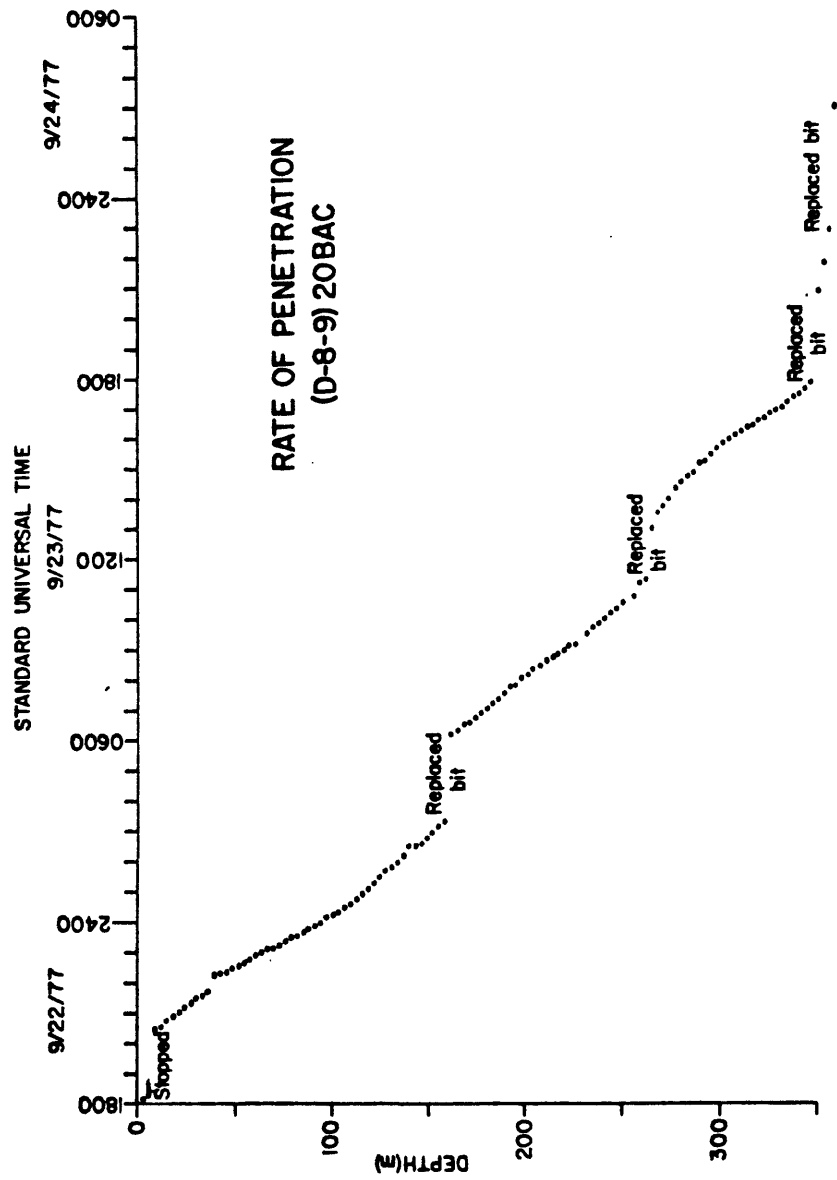
FIGURE 8.--Drilling penetration versus time, (D-8-9) 20BAC.
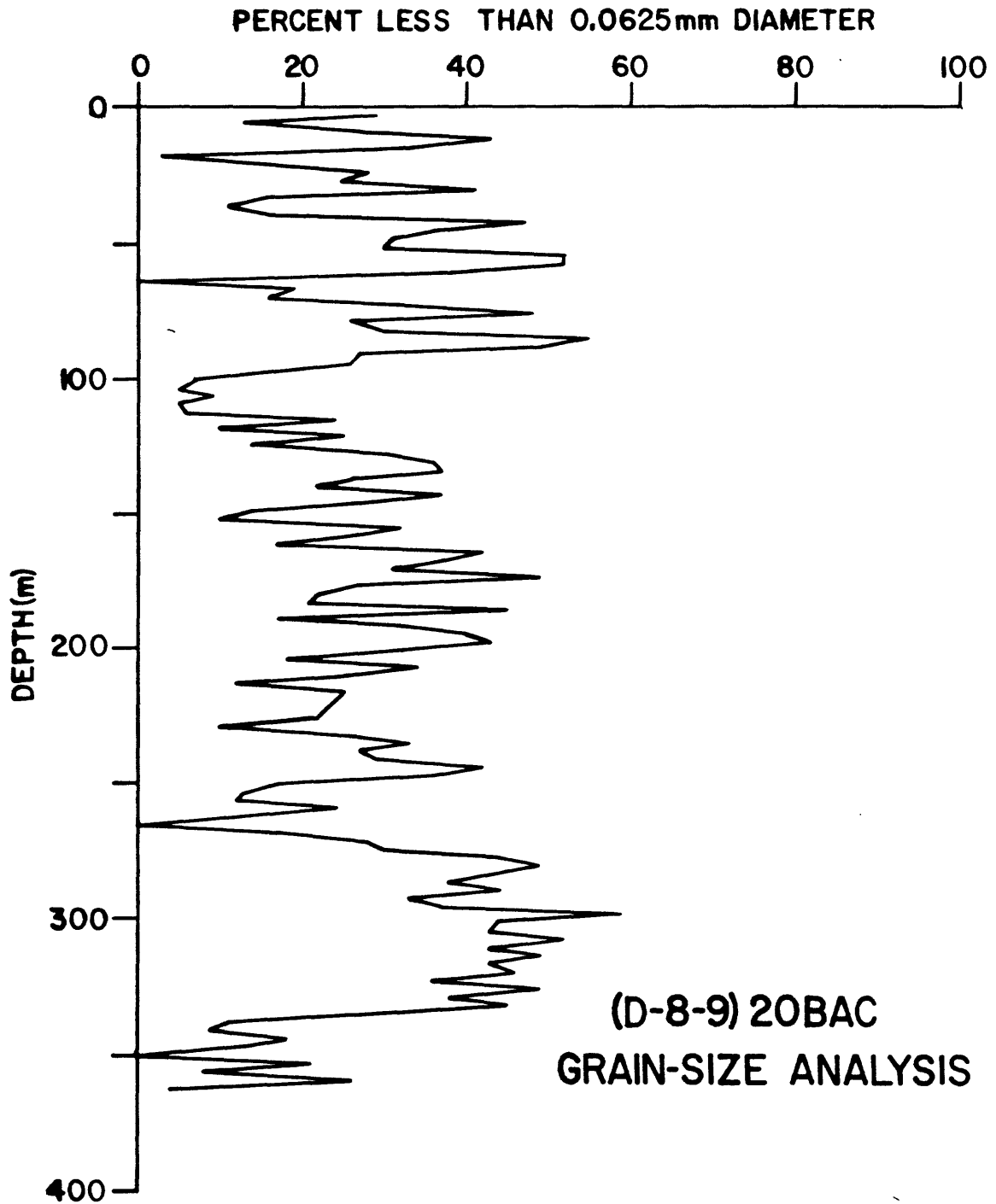
FIGURE 9.--Percent silt and clay in cuttings versus depth, (D-8-9) 20BAC.
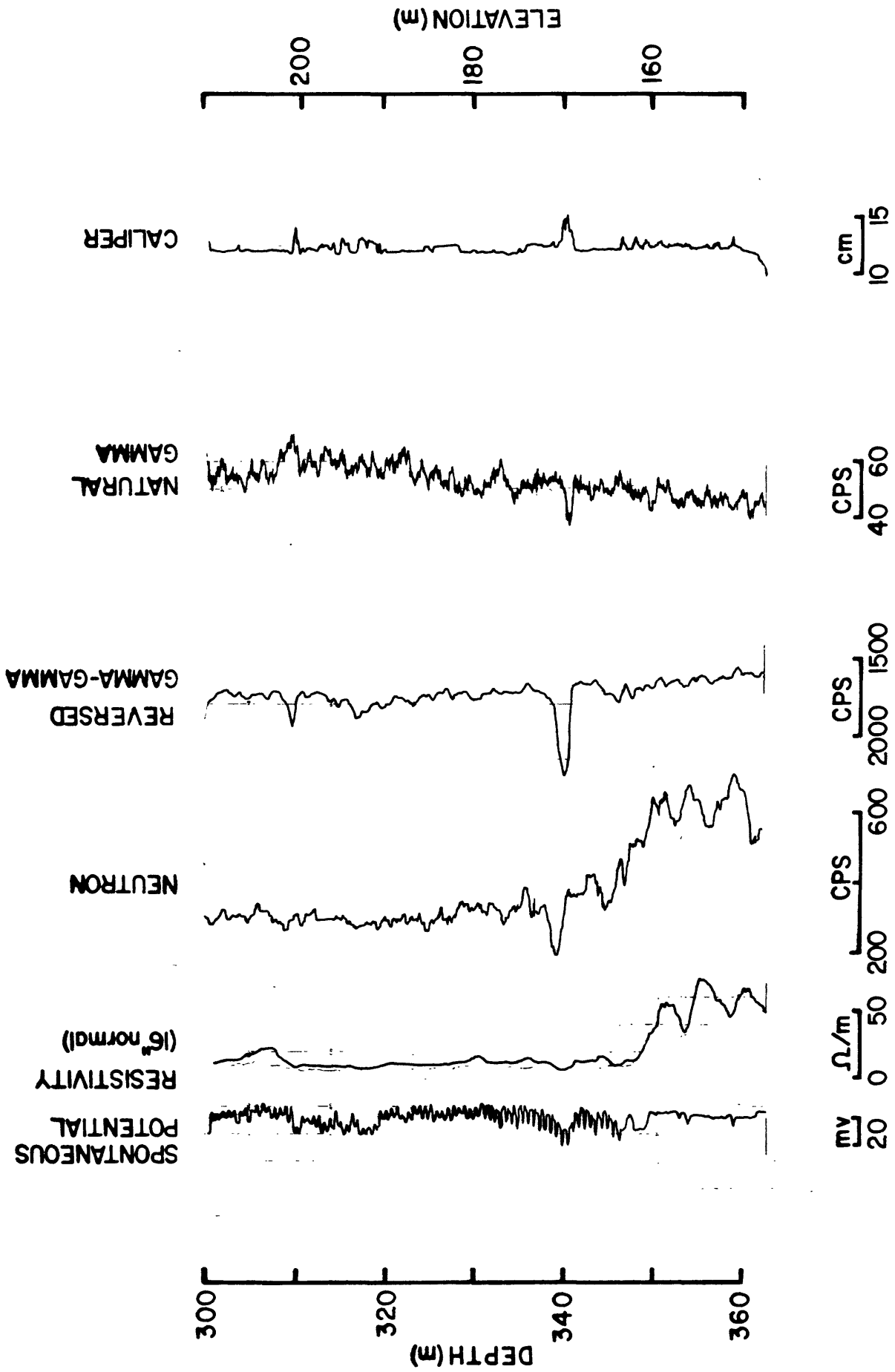
FIGURE 10.--Geophysical logs of lower part of (D-8-9) 20BAC.

27
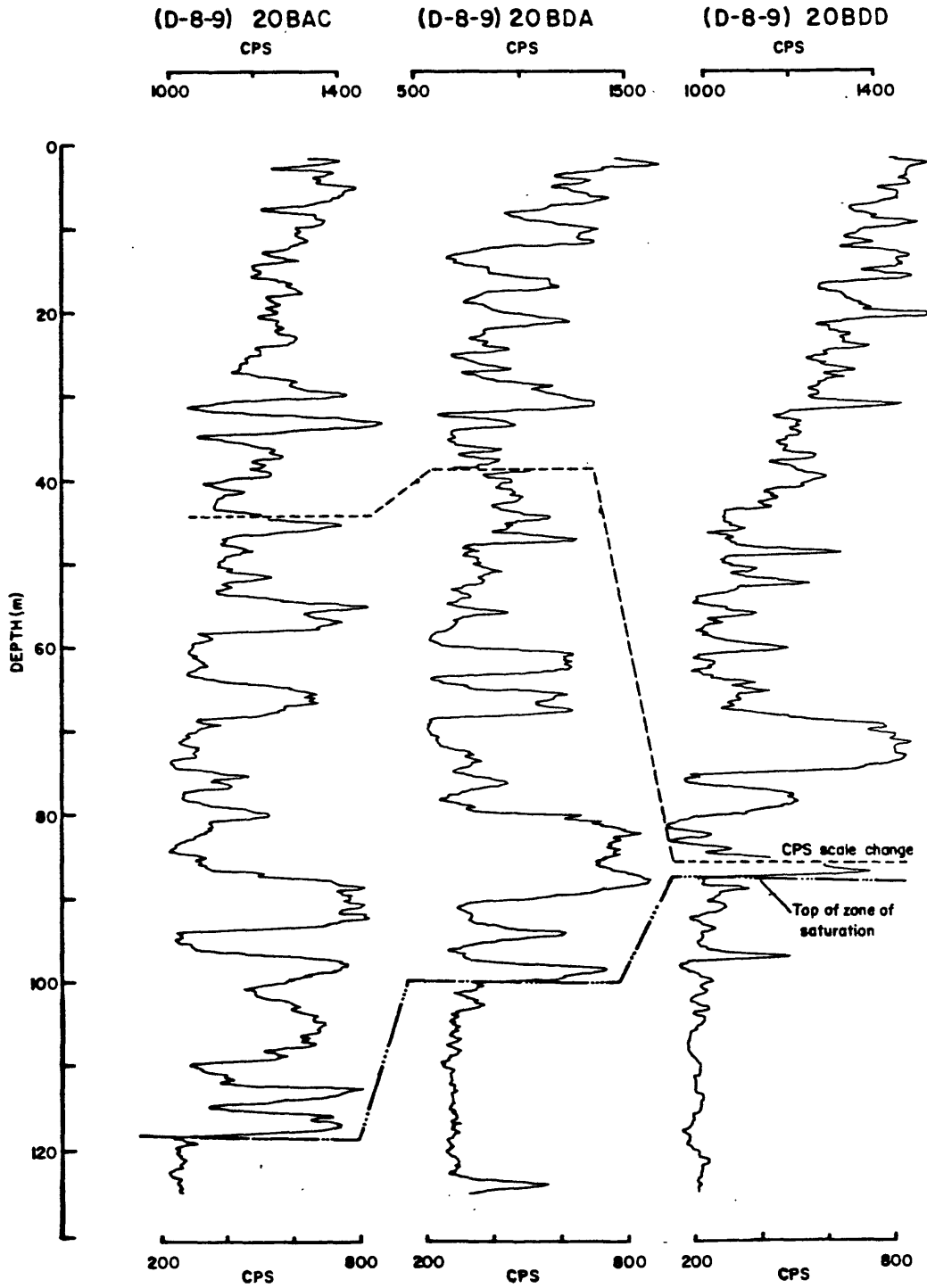
NEUTRON LOGS

FIGURE 11.--Neutron logs of unsaturated portions of test holes.
(CPS = counts per second.)

28
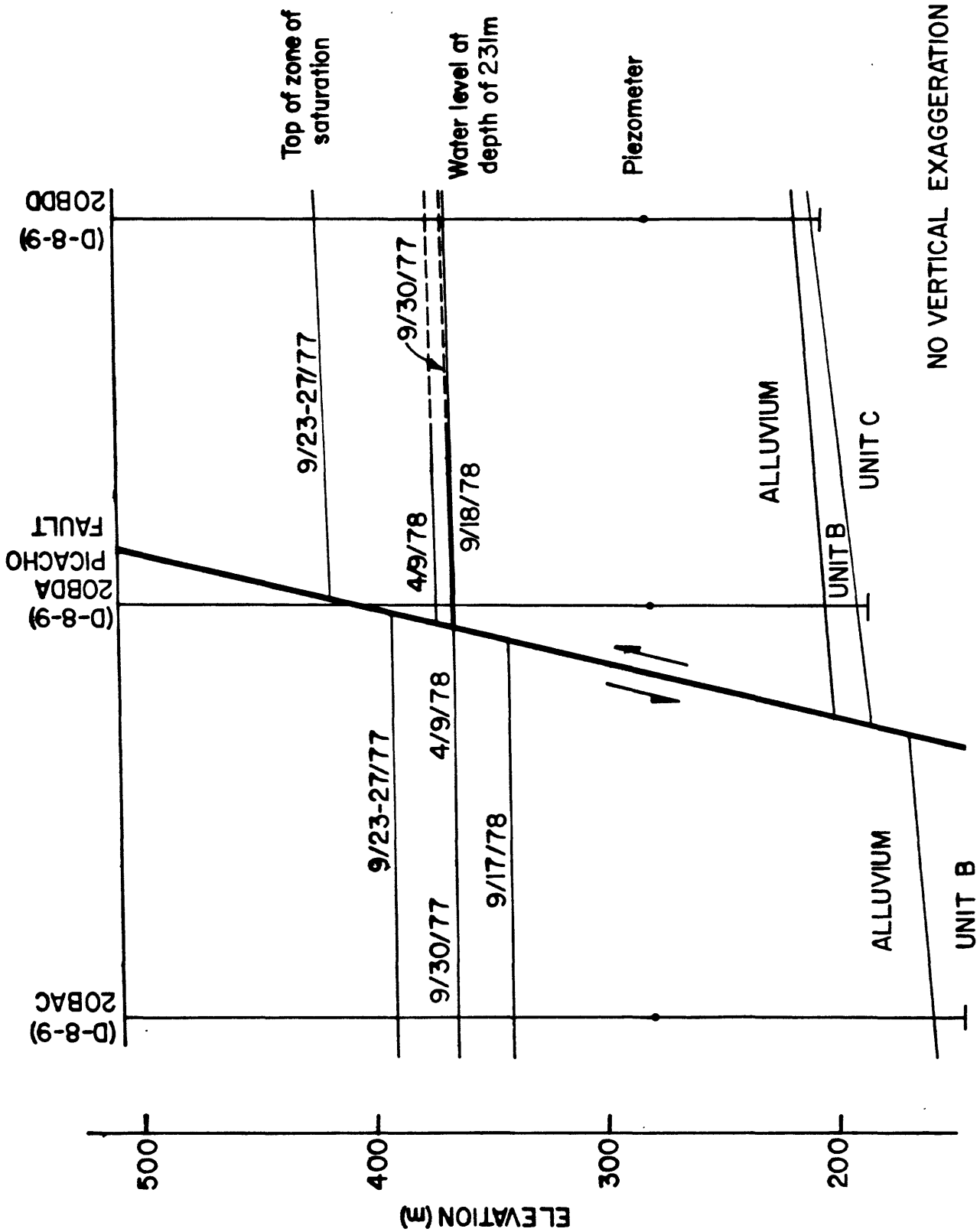
FIGURE 12.--Interpretive hydrogeologic cross section across Picacho fault. Water levels shown in cross section were measured in piezometers. Top of zone of saturation is from neutron logs.
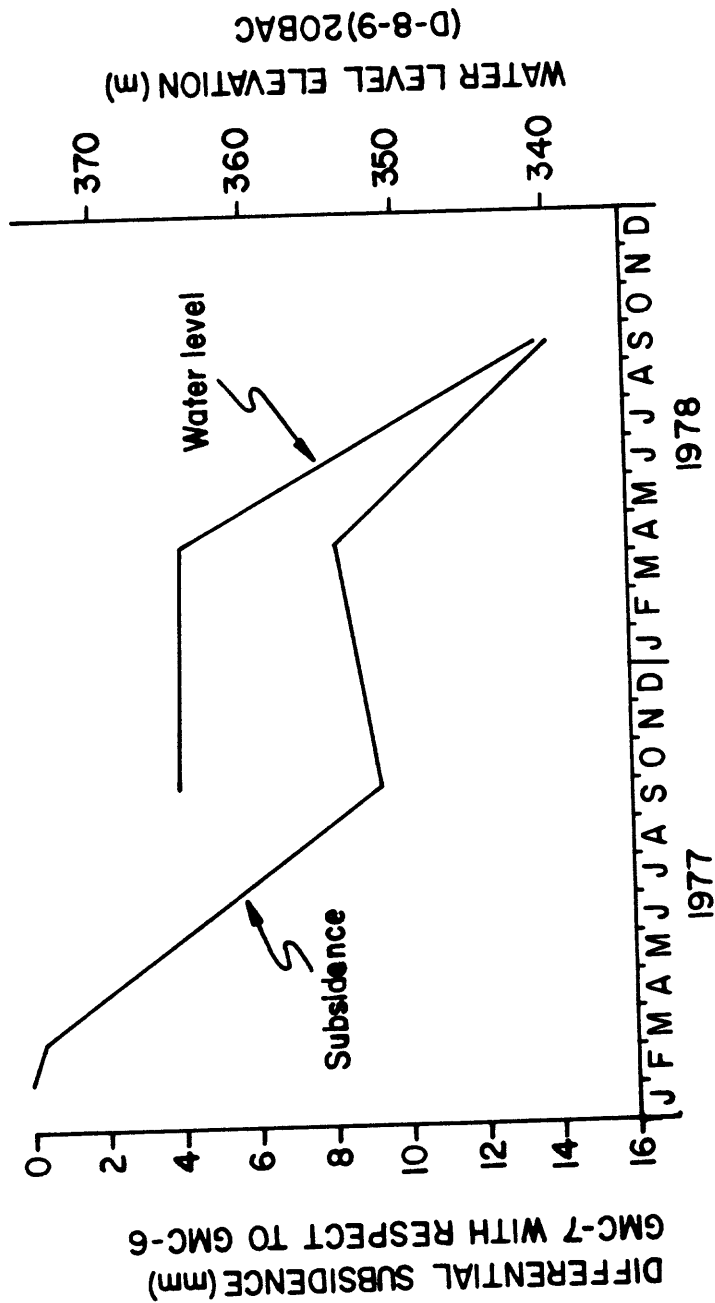
FIGURE 13.--Differential subsidence of bench marks 14.5 m apart on opposite sides of Picacho fault and elevation of water level in (D-8-9) 20BAC versus time. (See figure 1 for location of bench marks.)

Table 1.--Geotechnical properties of samples from cores of test hole (D-8-9) 20BDD

Depth interval cored (m)	Depth interval cored (ft)	Percent of core recovered	Part of core analyzed	Percent Particle Size (gradations in mm) <0.002	0.002-0.0625	0.0625-2.0	2.0-4.0	>4.0	Atterberg Limits Liquid Limit	Plastic Limit	Shrinkage Limit	Plasticity Index	Linear Shrinkage (per cent)	Unified Soil Classification Symbol	Composition (<2.0u) Illite	Kaolinite	Montmorillonite	Mixed layer
30.5 to 33.5	100 to 110	42	top	6.5	28.5	58.0	4.5	1.5	NP**	NP	28		8.5	SM	b		c	b
			middle	7.5	27.5	60.0	4.0	1.0	42	38	34	4	9.2	ML	b	c		c
			bottom	8.0	32.0	58.0	1.5	0.5	29	25	27	4	7.5	ML		c		a
45.7 to 48.8	150 to 160	65	top	10.5	56.5	32.0	0.5	0.5	37	28	29.7	9	10.3	ML	b		b	b
			middle	23.0	59.0	17.0	0.5	0.5	44	26	22.6	18	15.6	CL		c		a
			bottom	14.0	65.0	21.0	0.0	0.0	33	23	24.1	10	9.6	CL	b	c	a	c
61.0 to 64.0	200 to 210	9	top	17.0	43.0	34.0	2.0	4.0	36	19	21.5	17	12.3	CL	c	c		a
76.2 to 79.2	250 to 260	38	top(?)	23.0	41.5	33.5	1.5	0.5	38	21	20.6	17	15	CL	b	c	c	a
			middle(?)	33.5	32.5	32.5	1.0	0.5	44	29	21.9	15	18.3	ML	b	c	c	a
			bottom(?)	14.0	13.0	71.0	1.5	0.5	35.5	21.5	25.7	14	11.9	CL	c		b	b
91.4 to 94.5	300 to 310	77	top	11.5	33.0	54.5	0.5	0.5	28	20	22.4	8	8.1	CL	b		a	
			middle	16.5	54.0	28.5	0.5	0.5	35	26	22.6	9	12.4	ML			a	c
			bottom	18.0	44.0	36.0	1.5	0.5	31.5	22	22.3	9.5	10.3	CL	b		a	c
106.7 to 109.7	350 to 360	60	top	37.5	52.0	10.5	0.0	0.0	47	27	20.9	20	17.9	CL	b	c	c	a
			middle	21.0	71.0	8.0	0.0	0.0	36	22	21.6	14	11.8	CL	b	c	b	b
			bottom	30.0	54.0	16.0	0.0	0.0	42	23	22.2	19	15.6	CL	b		b	a
121.9 to 125.0	400 to 410	18	top	43.5	49.0	7.5	0.0	0.0	56	28	23.6	28	17.9	CH	c	c	b	b
			bottom	27.0	11.0	57.0	2.5	2.5	44	24	19.9	20	17.3	CL	b	c	b	b

*a-Primary mineral (40-60%); b-Secondary minerals (20-40%); c-Minor mineral (10-20%)

**NP = Not plastic

Table 2.--Grain-size distributions of cuttings from test holes

Test Hole		(D-8-9) 20BDD				(D-8-9) 20BDA				(D-8-9) 20BAC			
		Percentage of				Percentage of				Percentage of			
Sample Depth		Silt and clay <0.0625 mm	Sand >0.0625 mm	Gravel >2.0 mm	Gravel >4.0 mm	Silt and clay <0.0625 mm	Sand >0.0625 mm	Gravel >2.0 mm	Gravel >4.0 mm	Silt and clay <0.0625 mm	Sand >0.0625 mm	Gravel >2.0 mm	Gravel >4.0 mm
m	ft.												
3.0	10	23	22	20	35	29	27	24	20	33	24	24	19
6.1	20	23	36	21	20	13	28	34	25	17	28	28	27
9.1	30	32	40	12	16	27	36	14	23	19	28	35	18
12.2	40	32	31	24	13	43	34	15	8	20	42	18	20
15.2	50	26	22	39	13	33	33	14	20	30	31	25	14
18.3	60	39	24	14	23	3	18	14	65	22	24	32	22
21.3	70	2	31	24	43	15	20	19	46	29	35	19	17
24.4	80	32	31	23	14	28	29	18	25	25	20	25	30
27.4	90	21	42	19	18	25	36	15	24	23	34	15	28
30.5	100	33	29	19	19	41	35	10	14	23	19	23	35
33.5	110	35	34	17	14	16	18	19	47	9	36	22	33
36.6	120	31	26	16	27	11	6	24	59	23	25	15	37
39.6	130	28	39	14	19	16	16	15	53	18	40	21	21
42.7	140	32	37	12	19	47	30	13	10	27	35	22	16
45.7	150	23	18	20	39	36	27	15	22	27	19	29	25
48.8	160	8	82	2	8	31	31	11	27	21	32	15	32
51.8	170	8	69	15	8	30	30	10	30	30	27	18	25
54.9	180	9	60	17	14	52	30	7	11	53	29	8	10
57.9	190	58	21	4	17	52	16	11	21	52	29	9	10
61.0	200	58	28	6	8	38	13	28	21	55	26	10	9

32

Table 2.--Grain-size distributions of cuttings from test holes (continued)

| Sample Depth | | (D-8-9) 20BDD | | | | (D-8-9) 20BDA | | | | (D-8-9) 20BAC | | | |
| | | Percentage of | | | | Percentage of | | | | Percentage of | | | |
m	ft.	Silt and clay <0.0625 mm	Sand >0.0625 mm	Gravel >2.0 mm	Gravel >4.0 mm	Silt and clay <0.0625 mm	Sand >0.0625 mm	Gravel >2.0 mm	Gravel >4.0 mm	Silt and clay <0.0625 mm	Sand >0.0625 mm	Gravel >2.0 mm	Gravel >4.0 mm
64.0	210	31	47	11	11	0	15	39	46	18	21	34	27
67.1	220	37	48	8	7	19	22	17	42	32	28	22	18
70.1	230	60	27	7	6	16	13	19	52	19	18	33	30
73.2	240	20	36	19	25	32	22	18	28	12	19	32	37
76.2	250	28	27	29	16	48	20	11	21	20	46	23	11
79.2	260	18	47	17	18	26	24	9	41	46	29	12	13
82.3	270	19	51	21	9	30	31	16	13	11	41	38	10
85.3	280	60	22	9	9	55	22	9	14	19	16	43	22
88.4	290	42	37	10	11	49	29	9	13	0	11	36	53
91.4	300	28	26	21	25	27	31	16	26	25	19	34	22
94.5	310	27	39	13	21	26	14	32	28	7	20	20	53
97.5	320	48	31	14	7	17	7	16	60	12	13	29	46
100.6	330	39	35	20	6	7	17	24	52	2	24	32	42
103.6	340	45	33	14	8	5	21	40	34	19	10	45	26
106.7	350	52	29	11	8	9	20	27	44	5	11	32	52
109.7	360	16	65	12	7	5	16	25	54	22	21	18	39
112.8	370	42	29	9	11	6	13	20	61	10	23	33	34
115.8	380	59	26	6	9	24	20	28	28	17	21	24	38
118.9	390	40	40	13	7	10	27	33	30	43	26	13	18
121.9	400	53	33	8	6	25	26	17	32	56	20	8	16

33

Table 2.--Grain-size distributions of cuttings from test holes (continued)

Sample Depth		Test Hole (D-8-9) 20BDD Percentage of				(D-8-9) 20BDA Percentage of				(D-8-9) 20BAC Percentage of			
m	ft.	Silt and clay <0.0625 mm	Sand >0.0625 mm	Gravel >2.0 mm	Gravel >4.0 mm	Silt and clay <0.0625 mm	Sand >0.0625 mm	Gravel >2.0 mm	Gravel >4.0 mm	Silt and clay <0.0625 mm	Sand >0.0625 mm	Gravel >2.0 mm	Gravel >4.0 mm
125.0	410	44	32	15	9	14	24	25	37	39	33	9	19
128.0	420	63	24	6	7	30	44	15	11	50	24	14	12
131.1	430	63	26	5	6	36	36	13	15	37	21	18	24
134.1	440	66	17	9	8	37	43	10	10	61	19	11	9
137.2	450	65	25	5	5	26	49	16	9	52	29	11	8
140.2	460	55	19	7	19	22	43	15	20	59	25	6	10
143.3	470	25	34	34	7	37	44	12	7	48	32	10	10
146.3	480	27	48	17	8	26	22	17	35	49	27	13	11
149.4	490	52	29	11	8	14	24	44	18	26	38	24	12
152.4	500	52	28	13	7	10	22	47	21	43	25	18	14
155.4	510	44	30	15	11	18	32	36	14	32	31	23	14
158.5	520	38	38	15	9	26	54	13	7	29	27	28	16
161.5	530	42	30	23	5	17	24	31	28	13	52	22	13
164.6	540	50	34	9	7	42	27	13	18	36	38	15	11
167.6	550	44	40	10	6	37	40	17	6	41	37	10	12
170.7	560	41	38	11	10	31	34	17	18	31	45	15	9
173.7	570	44	30	16	10	49	31	12	8	31	41	16	12
176.8	580	24	44	26	6	27	38	25	10				
179.8	590	30	43	9	18	22	39	31	18	38	40	17	5
182.9	600	25	39	26	10	21	37	20	22				

Table 2.--Grain-size distributions of cuttings from test holes (continued)

Test Hole		(D-8-9) 20BDD				(D-8-9) 20BDA				(D-8-9) 20BAC			
		Percentage of				Percentage of				Percentage of			
Sample Depth		Silt and clay <0.0625 mm	Sand >0.0625 mm	Gravel >2.0 mm	Gravel >4.0 mm	Silt and clay <0.0625 mm	Sand >0.0625 mm	Gravel >2.0 mm	Gravel >4.0 mm	Silt and clay <0.0625 mm	Sand >0.0625 mm	Gravel >2.0 mm	Gravel >4.0 mm
m	ft.												
185.9	610	24	37	29	10	45	35	13	7	38	30	12	20
189.0	620	32	38	24	6	17	17	49	17	23	30	29	18
192.0	630	26	14	27	33	32	17	29	22	34	28	12	26
195.1	640	23	43	21	13	40	38	13	9	36	34	18	12
198.1	650	41	33	18	8	43	38	13	6	41	34	17	8
201.2	660	35	39	17	9	32	52	12	4	37	31	24	8
204.2	670	31	47	14	8	18	64	13	5	26	28	28	18
207.3	680	26	47	22	5	34	50	10	6	34	31	22	13
210.3	690	30	48	17	5	25	56	15	4	29	34	23	14
213.4	700	37	44	15	4	12	57	25	6	39	35	17	9
216.4	710	16	49	30	5	25	42	24	9	25	46	18	11
219.5	720	23	44	22	11	24	49	20	7	8	25	37	30
222.5	730	16	60	20	4	23	52	20	5	24	36	26	14
225.6	740	34	46	13	7	22	48	23	7	25	33	24	18
228.6	750	25	54	18	3	10	59	28	3	18	40	23	19
231.6	760	25	60	9	6	27	48	20	5	7	28	53	12
234.7	770	28	50	16	6	33	47	13	7	1	47	30	22
237.7	780	15	55	23	7	27	56	11	6	17	32	38	13
240.8	790	11	64	20	5	29	44	20	7	37	29	24	10
243.8	800	31	54	10	5	42	42	12	4	22	38	24	16

35

Table 2.--Grain-size distributions of cuttings from test holes (continued)

Test Hole			(D-8-9) 20BDD				(D-8-9) 20BDA				(D-8-9) 20BAC			
			Percentage of				Percentage of				Percentage of			
Sample Depth			Silt and clay <0.0625 mm	Sand >0.0625 mm	Gravel >2.0 mm	Gravel >4.0 mm	Silt and clay <0.0625 mm	Sand >0.0625 mm	Gravel >2.0 mm	Gravel >4.0 mm	Silt and clay <0.0625 mm	Sand >0.0625 mm	Gravel >2.0 mm	Gravel >4.0 mm
m	ft.													
246.9	810		24	53	17	6	36	49	8	7	11	46	31	12
249.9	820		66	34	18	12	17	60	16	7	14	32	34	20
253.0	830		41	42	13	4	13	56	24	7	8	40	33	19
256.0	840		23	29	39	9	12	32	51	5	23	38	26	13
259.1	850		21	55	19	5	24	43	27	6	20	40	31	9
262.1	860		30	32	34	4	13	51	26	10	10	29	47	14
265.2	870		21	25	40	14	0	15	22	63	18	40	22	20
268.2	880		23	30	37	10	17	33	25	25	42	26	18	14
271.3	890		36	26	29	9	28	41	24	7	24	35	33	8
274.3	900		37	47	14	2	30	46	16	8	40	31	20	9
277.4	910		29	32	29	10	44	40	11	5	38	33	19	10
280.4	920		9	28	20	43	49	36	11	4	35	33	24	8
283.5	930		17	34	38	11	43	40	13	4	35	26	22	17
286.5	940		32	34	28	6	38	40	15	7	19	18	46	17
289.6	950		32	47	17	4	44	39	13	4	22	30	31	17
292.6	960		17	50	28	5	33	49	14	4	21	27	40	12
295.7	970		13	42	39	6	37	36	20	7	6	29	47	18
298.7	980		17	29	45	9	59	28	10	3	31	27	28	14
301.8	990		7	52	37	4	44	37	12	7	6	18	43	33
304.8	1000		4	82	9	5	43	35	15	7	28	27	35	10

36

Table 2.--Grain-size distributions of cuttings of test holes (continued)

| Sample Depth | | (D-8-9) 20BDD | | | | (D-8-9) 20BDA | | | | (D-8-9) 20BAC | | | |
| m | ft. | Silt and clay <0.0625 mm | Sand >0.0625 mm | Gravel >2.0 mm | Gravel >4.0 mm | Silt and clay <0.0625 mm | Sand >0.0625 mm | Gravel >2.0 mm | Gravel >4.0 mm | Silt and clay <0.0625 mm | Sand >0.0625 mm | Gravel >2.0 mm | Gravel >4.0 mm |
		Percentage of				Percentage of				Percentage of			
307.8	1010					52	35	9	4	13	26	47	14
310.9	1020					43	42	11	4	14	34	30	22
313.9	1030					43	32	19	6	29	28	37	6
317.0	1040					49	33	10	8	1	37	40	22
320.0	1050					46	34	13	7	17	36	28	19
323.1	1060					36	41	15	8	2	71	24	3
326.1	1070					49	35	11	5				
329.2	1080					38	42	15	5				
332.2	1090					45	41	10	4				
335.3	1100					29	39	27	5				
338.3	1110					11	48	25	6				
341.4	1120					9	49	34	8				
344.4	1130					18	49	28	5				
347.5	1140					13	43	41	3				
350.5	1150					0	15	23	62				
353.6	1160					21	33	28	18				
356.6	1170					8	79	6	7				
359.7	1180					26	40	21	13				
362.7	1190					4	51	41	4				

37

Table 3.—Hydrologic Data

Test Hole	(D-8-9) 20BAC	(D-8-9) 20BDA	(D-8-9) 20BDD
	Depth/Elevation (m)	Depth/Elevation (m)	Depth/Elevation (m)
Top of Zone of Saturation, Neutron Log			
September 23-27, 1977	118.26/391.43	99.97/412.44	87.48/427.93
Water Level in piezometer			
September 30, 1977	144.70/364.99	143.07/369.34	plugged
April 9, 1978	145.15/364.54	136.65/375.76	plugged
September 17-18, 1978	168.76/340.93	144.09/368.32	141.99/373.42
Top of well screen	230.92/278.77	230.18/282.23	231.27/284.14
Base of well screen	232.44/277.25	231.70/280.71	232.79/282.62
Land Surface	--- /509.69	--- /512.41	--- /515.41